HHS Public Access

Author manuscript

Nat Cell Biol. Author manuscript; available in PMC 2011 April 01.

Published in final edited form as:

Nat Cell Biol. 2010 October ; 12(10): 999–1006. doi:10.1038/ncb2101.

Prdm16 promotes stem cell maintenance in multiple tissues, partly by regulating oxidative stress

Sergei Chuikov[1,*], **Boaz P. Levi**[1,*], **Michael L. Smith**[1], and **Sean J. Morrison**[1,2]

[1] Howard Hughes Medical Institute, Department of Internal Medicine, and Center for Stem Cell Biology, Life Sciences Institute, University of Michigan, Ann Arbor, Michigan, 48109-2216

Abstract

To better understand the mechanisms that regulate stem cell identity and function we sought to identify genes that are preferentially expressed by stem cells and critical for their function in multiple tissues. Prdm16 is a transcription factor that regulates leukemogenesis[1], palatogenesis[2], and brown fat development[3]–[5], but which was not known to be required for stem cell function. We demonstrate that *Prdm16* is preferentially expressed by stem cells throughout the nervous and hematopoietic systems and required for their maintenance. *Prdm16* deficiency led to changes in reactive oxygen species (ROS) levels, increased cell death, altered cell cycle distribution, and stem cell depletion in the hematopoietic and nervous systems. In neural stem/progenitor cells, Prdm16 bound the *Hgf* promoter and in the absence of *Prdm16 Hgf* expression declined. Addition of recombinant HGF to culture partially rescued the increase in ROS levels and the depletion of *Prdm16* deficient neural stem cells. Administration of the anti-oxidant, N-acetyl-cysteine, to *Prdm16* deficient mice partially rescued defects in neural stem/progenitor cell function and neural development. Prdm16 therefore promotes stem cell maintenance in multiple tissues, partly by modulating oxidative stress.

The development and maintenance of vertebrate tissues depends upon diverse stem cells. Stem cells are functionally distinct from downstream progenitors and likely depend upon regulatory mechanisms that are conserved among stem cells from different tissues but are absent in most downstream progenitors[6]. Yet few such mechanisms have been identified. FoxO family transcription factors[7]–[10], polycomb family (e.g. Bmi-1) epigenetic regulators[11], and DNA repair genes[12] are required for the maintenance of stem cells in multiple tissues but are widely expressed within tissues and likely to regulate many cells. Other genes, like *Evi1*[13] and *Sox17*[14], are preferentially expressed by stem cells and required for stem cell maintenance in one tissue (in this case the hematopoietic system) but are not

[2]Correspondence: 5435 Life Sciences Institute, 210 Washtenaw Ave., Ann Arbor, Michigan, 48109-2216; phone 734-647-6261; fax 734-615-8133; seanjm@umich.edu.

*These authors contributed equally

AUTHOR CONTRIBUTION

SC and BPL characterized *Prdm16* expression and function with assistance from MLS. SC, BPL, and SJM designed experiments, interpreted results, and wrote the manuscript.

COMPETING FINANCIAL INTERESTS

The authors are not aware of any competing financial interests.

known to regulate stem cells in other tissues. Other genes, like Lgr5[15, 16], are preferentially expressed by stem cells in multiple tissues but it is unknown whether they regulate stem cell function. The identification of genes that are preferentially expressed by stem cells and required to maintain stem cells in multiple tissues would therefore provide important new insights into stem cell identity and function.

To identify genes that regulate the self-renewal of diverse stem cells we performed a Bmi-1 suppressor screen by transposon mutagenesis (data not shown). We reasoned that by screening for suppressors of the *Bmi-1* deficiency phenotype we could identify genes that modulate a widely used self-renewal pathway and that might encode new self-renewal regulators required by diverse stem cells. Our screen revealed that over-expression of *Prdm16* partially restored the ability of *Bmi-1* deficient hematopoietic cells to reconstitute irradiated mice (data not shown). *Prdm16* over-expression can contribute to leukemogenesis[1, 17] and can increase the ability of cultured hematopoietic stem cells (HSCs) to reconstitute irradiated mice[18], though no study has addressed whether *Prdm16* is required for stem cell function in any tissue. We decided to test whether *Prdm16*, like *Bmi-1*, is physiologically required for stem cell function in multiple tissues.

We reanalyzed previously published gene expression profile data[19] and found that *Prdm16* was expressed by highly purified HSCs and transiently reconstituting multipotent hematopoietic progenitors (MPPs) but was not detectable in unfractionated hematopoietic cells (Fig. 1a). Quantitative RT-PCR (qPCR) in independent samples yielded similar results as *Prdm16* was expressed at 100-fold higher levels in highly purified $CD150^{+}CD41^{-}CD48^{-}Sca1^{+}c\text{-}kit^{+}$ HSCs[19] as compared to unfractionated bone marrow cells (Fig. 1b).

To evaluate *Prdm16* expression at the single cell level we used $Prdm16^{Gt(OST67423)Lex}$ (further referred to as $Prdm16^{LacZ}$) genetrap mice in which *LacZ* was inserted into the first intron of *Prdm16*[2]. This allele allowed us to assess *Prdm16* expression based on β-galactosidase activity but terminated *Prdm16* translation after the first exon, causing a loss of *Prdm16* function[2]. Based on staining with the fluorogenic β-galactosidase substrate fluorescein di-β-D-galactopyranoside (FDG), less than 3% of $Prdm16^{LacZ/+}$ bone marrow cells had β-galactosidase activity (Fig. 1c–d). Most β-galactosidase+ cells were $c\text{-}kit^{+}$ and $Sca\text{-}1^{+}$, markers of HSCs and other primitive progenitors. 61±7% of all $c\text{-}kit^{+}Sca1^{+}$ bone marrow cells were β-galactosidase+ in $Prdm16^{LacZ/+}$ mice (Fig. 1d). Almost all $CD150^{+}CD41^{-}CD48^{-}Sca1^{+}c\text{-}kit^{+}$ HSCs[19] (90±10%) and $CD150^{-}CD41^{-}CD48^{-}Sca1^{+}c\text{-}kit^{+}$ MPPs[20] (82±2%) from 2 month-old $Prdm16^{LacZ/+}$ mice expressed β-galactosidase by flow-cytometry (Fig. 1d, e). In contrast, differentiated B, myeloid, T, and erythroid cells rarely expressed β-galactosidase (Fig. 1d). β-galactosidase+ cells from the bone marrow of 2 month-old $Prdm16^{LacZ/+}$ mice contained nearly all of the colony-forming cells (CFU-Cs; 0.7±0.2% of bone marrow cells) in $Prdm16^{LacZ/+}$ bone marrow (Fig. 1f). *Prdm16* is thus preferentially expressed by HSCs and other primitive progenitors in the hematopoietic system.

Prdm16 was also preferentially expressed by stem cells in the nervous system. In forebrain sections from adult $Prdm16^{LacZ/+}$ mice, β-galactosidase strongly overlapped with the stem/

progenitor cell marker, Nestin, in the lateral ventricle subventricular zone (SVZ) but much less β-galactosidase staining was observed among the differentiated cells in the striatum and cortex (Fig. 1i–l). Similar results were observed in the newborn forebrain where β-galactosidase overlapped with Nestin in the lateral ventricle ventricular zone (VZ) (Suppl. Fig. 1). Virtually all neurospheres cultured from the *Prdm16*$^{LacZ/+}$, but not *Prdm16*$^{+/+}$, forebrain exhibited strong β-galactosidase staining (Fig. 1g–h). Cultured and uncultured neural crest stem cells from the enteric nervous system also expressed *Prdm16* (Suppl. Fig. 2). *Prdm16* is therefore expressed by neural stem/progenitor cells in the central and peripheral nervous systems but expression declines as these cells differentiate.

We next tested whether *Prdm16* is required to regulate HSCs. *Prdm16*$^{LacZ/LacZ}$ mice were born at Mendelian frequency but died soon after birth (Suppl. Fig. 3a, b). Hematopoiesis was grossly normal in newborn *Prdm16*$^{LacZ/LacZ}$ mice as liver and spleen cellularity were normal (Fig. 2a). No significant differences were detected in the frequency of myeloid, B, or T cells in the livers or spleens of newborn *Prdm16*$^{LacZ/LacZ}$, *Prdm16*$^{LacZ/+}$, and *Prdm16*$^{+/+}$ mice (Fig 2b, Suppl. Fig. 3c). Most colony-forming progenitors were present at normal frequencies in the neonatal liver of *Prdm16*$^{LacZ/LacZ}$ mice (Fig. 2c). However, mixed myeloerythroid (CFU-GEMM) and mixed myeloid (CFU-GM) progenitors were significantly depleted in the livers of neonatal *Prdm16*$^{LacZ/LacZ}$ mice (Fig. 2c). The frequency of CD150^{+}CD41^{-}CD48^{-}Sca1^{+}c-kit^{+} HSCs in the embryonic day (E)14.5 liver (Fig. 2d), newborn (P0) liver (Fig. 2d–e), and newborn spleen (Suppl. Fig. 3d) was reduced by approximately 2-fold in *Prdm16*$^{LacZ/+}$ mice and by approximately 20-fold in *Prdm16*$^{LacZ/LacZ}$ mice compared to *Prdm16*$^{+/+}$ littermates. Loss of *Prdm16* therefore profoundly depletes HSCs without depleting most downstream hematopoietic progenitors.

To assess HSC function we performed competitive long-term reconstitution assays using neonatal liver cells from *Prdm16*$^{LacZ/LacZ}$ mice and littermate controls. 300,000 donor (CD45.2^{+}) *Prdm16*$^{+/+}$ cells or *Prdm16*$^{LacZ/+}$ cells gave long-term multilineage reconstitution by myeloid, B, and T cells in all irradiated recipient (CD45.1^{+}) mice (Fig. 2f). In contrast, 300,000 *Prdm16*$^{LacZ/LacZ}$ cells did not give long-term multilineage reconstitution in any recipients. All recipients of *Prdm16*$^{LacZ/LacZ}$ cells had low levels of transient reconstitution by donor B cells, and most had very low levels of transient myeloid or T cell reconstitution (Fig. 2f).

Since *Prdm16*$^{LacZ/LacZ}$ mice exhibited a 20-fold depletion of HSCs (Fig. 2d), we performed an additional experiment in which a 20-fold excess of donor (CD45.2^{+}) cells from newborn *Prdm16*$^{LacZ/LacZ}$ mice was transplanted into irradiated wild-type recipients (CD45.1^{+}) along with 300,000 recipient bone marrow cells. As in prior experiments, 300,000 *Prdm16*$^{LacZ/LacZ}$ cells gave poor reconstitution in all lineages while 300,000 *Prdm16*$^{+/+}$ cells gave long-term multilineage reconstitution in all recipients (Fig. 2g). 6×10^{6} neonatal *Prdm16*$^{LacZ/LacZ}$ liver cells gave long-term multilineage reconstitution in all recipients, but the levels of donor cell reconstitution were significantly lower than from 300,000 *Prdm16*$^{+/+}$ control cells and were declining by 16 weeks after transplantation (Fig. 2g). Some HSC activity thus remains in newborn *Prdm16*$^{LacZ/LacZ}$ mice, and can sustain hematopoiesis, but these HSCs are greatly depleted.

To further test whether the residual *Prdm16*$^{LacZ/LacZ}$ HSCs were defective we transplanted 20 CD150^{+}CD41^{-}CD48^{-}Sca1^{+}c-kit^{+} HSCs from *Prdm16*$^{LacZ/LacZ}$, *Prdm16*$^{LacZ/+}$, or *Prdm16*$^{+/+}$ neonates into irradiated recipients along with 300,000 recipient bone marrow cells. Four of 10 recipients of *Prdm16*$^{+/+}$ HSCs and 6 of 10 recipients of *Prdm16*$^{LacZ/+}$ HSCs, but none of 9 recipients of *Prdm16*$^{Lacz/LacZ}$ HSCs, were long-term multilineage reconstituted (Fig. 2h). The levels of donor cell reconstitution by *Prdm16*$^{Lacz/LacZ}$ HSCs were significantly lower than from control HSCs in all lineages (Fig. 2h). Even highly enriched HSC populations therefore have little reconstituting capacity in the absence of *Prdm16*. Furthermore, the frequency of HSCs in adult *Prdm16*$^{LacZ/+}$ bone marrow was significantly reduced (3-fold) relative to *Prdm16*$^{+/+}$ bone marrow (Fig. 2i). *Prdm16* is therefore required for the maintenance of fetal and adult HSCs.

Prdm16 is required for normal cell cycle regulation and survival in HSCs and other primitive hematopoietic progenitors. *Prdm16* deficiency significantly increased the frequency of c-kit^{+}Sca-1^{+} cells, but not unfractionated liver cells, that stained positively for AnnexinV and DAPI (Fig. 2j; we could not evaluate highly purified HSCs in this assay because they were too rare in *Prdm16*$^{Lacz/LacZ}$ mice). *Prdm16* deficiency also significantly increased the frequency of c-kit^{+}Sca-1^{+} cells, but not unfractionated liver cells, that stained positively for activated caspase-3 (data not shown). *Prdm16* deficiency significantly increased the frequency of HSCs, MPPs, and c-kit+Sca-1+ cells, but not unfractionated liver cells, in S/G2/M phase of the cell cycle (Fig. 2k).

Prdm16 also regulates neural development. Brain mass was significantly reduced in *Prdm16*$^{LacZ/LacZ}$ mice compared to littermate controls (Fig. 3a). *Prdm16*$^{LacZ/LacZ}$ forebrains had a thinner cortex (see brackets in Fig. 3c versus 3b), narrower ventricles (see arrowheads in Fig. 3c versus 3b), and agenesis of the corpus callosum (see arrows in Fig. 3c versus 3b, confirmed by serial sections). Axons in *Prdm16*$^{LacZ/LacZ}$ mice formed Probst bundles[21] instead of crossing the midline (see * in Fig. 3e; see arrows in Fig. 3d versus 3e).

To test whether *Prdm16* regulates neural stem cell function we cultured VZ cells from newborn *Prdm16*$^{LacZ/LacZ}$ mice and littermate controls at clonal densities (<1 cell/μl). *Prdm16*$^{LacZ/LacZ}$ VZ cells formed neurospheres that underwent multilineage differentiation (Fig. 3f, g). However, the frequency of VZ cells that formed multilineage colonies in culture was significantly reduced in *Prdm16*$^{LacZ/LacZ}$ mice (Fig. 3h). *Prdm16*$^{LacZ/LacZ}$ neurospheres were also significantly smaller than *Prdm16*$^{+/+}$ and *Prdm16*$^{LacZ/+}$ neurospheres (Fig. 3i). The self-renewal potential of *Prdm16*$^{LacZ/LacZ}$ neural stem cells was significantly less than control stem cells based on the number of multipotent daughter cells that could be subcloned from individual primary neurospheres (Fig. 3j). *Prdm16* was similarly required for stem cell function in the peripheral nervous system (Suppl. Fig. 2c,d). *Prdm16* deficiency thus reduces self-renewal potential and depletes neural stem cells, similar to the defects observed in the hematopoietic system.

To test whether we could observe neural stem/progenitor cell defects in vivo we stained sections through the forebrain of newborn *Prdm16*$^{LacZ/LacZ}$ mice and littermate controls with an antibody against phospho-Histone3 (pH3) to identify mitotic cells. We observed significantly fewer pH3+ cells in the lateral ventricle VZ of *Prdm16*$^{LacZ/LacZ}$ mice compared

to littermate controls (Fig. 3k–o). We also observed a significantly increased frequency of activated caspase-3+ cells among *Prdm16*$^{LacZ/LacZ}$ VZ cells (Fig. 3p–r). These effects were more pronounced in the dorsal VZ than in the ventral VZ. *Prdm16* is therefore required for normal cell cycle regulation and survival in neural stem/progenitor cells.

To investigate the underlying mechanisms we compared the gene expression profiles of uncultured VZ cells from newborn *Prdm16*$^{LacZ/LacZ}$, *Prdm16*$^{LacZ/+}$, and *Prdm16*$^{+/+}$ mice (3 independent samples per genotype). Thirteen genes were significantly reduced in expression (Fig 4a) and six were significantly increased in expression (Suppl. Fig. 3e) in the *Prdm16*$^{LacZ/LacZ}$ VZ (at least 2.2-fold different ($p<0.05$) between *Prdm16*$^{LacZ/LacZ}$ and *Prdm16*$^{+/+}$ VZ and at least 1.8-fold different ($p<0.05$) between *Prdm16*$^{LacZ/LacZ}$ and *Prdm16*$^{LacZ/+}$ VZ). These differences were confirmed by qPCR in 3 independent samples per genotype (Fig. 4a; Suppl. Fig. 3e). Several of these genes regulate the generation of ROS or the response to oxidative stress (see * in Fig. 4a). In particular, *Hepatocyte growth factor* (*Hgf*), and *Metallothienin2* (*Mt2*) expression were reduced in *Prdm16*$^{LacZ/LacZ}$ VZ (Fig. 4a). The reduction in *Hgf* expression in the absence of *Prdm16* was further confirmed in neurospheres cultured from the newborn VZ (Fig. 4b). These changes would be predicted to increase ROS levels as MT2 scavenges free radicals[22] and HGF can protect cells from oxidative stress by reducing ROS levels[23], [24]. *Metallothionein1* (*Mt1*) expression was also reduced in the *Prdm16*$^{LacZ/LacZ}$ VZ (1.7-fold by microarray and 3.7-fold by qPCR; data not shown). Consistent with these predictions, DCFDA staining (an indicator of ROS levels) significantly increased in newborn *Prdm16*$^{LacZ/LacZ}$ VZ cells as compared to littermate controls (Fig. 4c–d). Although *Prdm16*$^{LacZ/LacZ}$ VZ cells had increased ROS levels, we did not detect any defects in mitochondrial mass or membrane potential (Suppl. Fig. 4c, d). *Prdm16* is therefore required to control the expression of genes that regulate ROS levels in neural stem/progenitor cells and to avoid oxidative stress.

Chromatin immunoprecipitation experiments were conducted to test if Prdm16 directly binds the promoters of *Hgf* and *Mt2*. Two of four sequences 5′ of the *Hgf* start codon were immunoprecipitated from *Prdm16*$^{+/+}$, but not *Prdm16*$^{LacZ/LacZ}$, neurospheres using anti-Prdm16 antibodies (Fig 4e). In contrast, no Prdm16 binding was detected at the *Mt2* promoter. These data suggest that *Hgf*, but not *Mt2*, is a direct target of Prdm16.

To test whether HGF regulates oxidative stress in neural stem/progenitor cells we added recombinant HGF to neurospheres cultured from the VZ of newborn *Prdm16*$^{LacZ/LacZ}$ mice and littermate controls. The *Prdm16*$^{LacZ/LacZ}$ cells exhibited significantly higher levels of DCFDA staining but HGF treatment significantly reduced DCFDA staining in these cells (Fig. 4f). These data suggest that HGF regulates ROS levels in neural stem/progenitor cells and that Prdm16 regulates oxidative stress in neural stem/progenitor cells partly by regulating Hgf expression.

To test whether oxidative stress contributed to the defects in neural stem/progenitor cell function and neural development we administered the anti-oxidant N-acetyl-cysteine (NAC) to pregnant *Prdm16*$^{LacZ/+}$ mice. NAC significantly increased brain size in newborn *Prdm16*$^{LacZ/LacZ}$ mice (Fig. 5a, b) but did not affect brain size in *Prdm16*$^{LacZ/+}$ or *Prdm16*$^{+/+}$ mice (Fig 5b). In wild-type mice, glial fibrillary acidic protein (GFAP)

expressing astrocytes were evident around the midline and the corpus callosum at birth (Fig. 5c) but many fewer GFAP+ cells were observed around the midline of *Prdm16*$^{LacZ/LacZ}$ mice (Fig. 5d). *Prdm16*$^{LacZ/LacZ}$ mice treated with NAC in utero had more GFAP+ cells around the midline in the forebrain (Fig. 5e), though the corpus callosum still did not develop in these mice. NAC treatment in utero (Fig 5f) or in culture (Fig. 5g) also significantly increased the frequency of newborn *Prdm16*$^{LacZ/LacZ}$ VZ cells, but not *Prdm16*$^{LacZ/+}$ or *Prdm16*$^{+/+}$ VZ cells, that formed multipotent neurospheres in culture. Oxidative stress therefore contributes to the defects in neural development in *Prdm16*$^{LacZ/LacZ}$ mice.

Since Prdm16 promotes *Hgf* expression in neural stem/progenitor cells (Fig. 4a,b,e), HGF regulates ROS levels in these cells (Fig. 4f), and increased ROS levels contribute to the defects in neural stem/progenitor cell function in *Prdm16*$^{LacZ/LacZ}$ mice (Fig. 5), we tested whether addition of HGF to culture could partially rescue the defects in *Prdm16*$^{LacZ/LacZ}$ neural stem cell function. Addition of HGF significantly increased the frequency of *Prdm16*$^{LacZ/LacZ}$, but not *Prdm16*$^{LacZ/+}$ or *Prdm16*$^{+/+}$, VZ cells that formed multipotent neurospheres (Fig. 5h).

To test whether loss of *Prdm16* changes ROS levels within primitive hematopoietic progenitors, we stained c-kit^{+}Sca-1^{+} stem/progenitor cells from newborn *Prdm16*$^{LacZ/LacZ}$ mice with DCFDA. Surprisingly, we observed a significant decline in ROS levels within *Prdm16*$^{LacZ/LacZ}$ c-kit^{+}Sca-1^{+} liver cells compared to control cells while ROS levels remained unchanged in unfractionated liver cells (Suppl. Fig. 4a–b). Thus, *Prdm16* is also required to regulate ROS levels in primitive hematopoietic progenitors, though loss of *Prdm16* appeared to decrease ROS levels in these cells, in contrast to the nervous system. Furthermore, NAC treatment of pregnant mice did not rescue the depletion of CD150^{+}CD41^{-}CD48^{-}Sca1^{+}c-kit^{+} HSCs in *Prdm16*$^{LacZ/+}$ or *Prdm16*$^{LacZ/LacZ}$ mice (Fig. 5i). Prdm16 might promote stem cell maintenance by different mechanisms in different tissues. Alternatively, there could be an increase in ROS levels in *Prdm16*$^{LacZ/LacZ}$ HSCs that is masked by other changes that occur among the heterogeneous c-kit^{+}Sca-1^{+} cells. Unfortunately, this is impossible to test because too few HSCs can be recovered from *Prdm16*$^{LacZ/LacZ}$ mice (Fig. 2d) to assess DCFDA staining. In either case, the failure of NAC to rescue the depletion of *Prdm16*$^{LacZ/LacZ}$ HSCs suggests that Prdm16 has other critical functions in HSCs beyond regulating oxidative stress. Finally, compensatory changes might also be induced in response to oxidative stress[25] in either HSCs or neural stem/progenitor cells that alter the observed effects of *Prdm16* deficiency on ROS levels.

Our results demonstrate that Prdm16 is required for stem cell function in the nervous and hematopoietic systems (Fig. 2, 3). In the central nervous system, Prdm16 appears to promote neural stem/progenitor cell function partly by promoting HGF expression (Fig. 4a,b,e) and regulating ROS levels (Fig. 4f). However, Prdm16 likely regulates ROS levels and stem cell maintenance by other mechanisms as well. Our results emphasize the critical and diverse mechanisms required by stem cells to regulate oxidative stress. *Bmi-1* also regulates ROS levels in stem cells[26], but Prdm16 does not appear to regulate *Bmi-1* expression or vice versa (data not shown). Considerable additional work will be required to fully elucidate the mechanisms by which Prdm16 regulates oxidative stress and stem cell maintenance.

METHODS

Mice

Prdm16$^{Gt(OST67423)Lex}$ genetrap mice were obtained from the NIH Mutant Mouse Regional Resource Center (http://www.mmrrc.org/). C57BL/Ka-CD45.1:Thy-1.2 mice were recipients in reconstitution experiments. All mice were backcrossed onto a C57BL/Ka background.

Reconstitution assay

Single cell suspensions of liver cells from neonatal mice were transplanted into recipient mice by retro-orbital venous sinus injection. Eight week-old recipient mice were irradiated in two doses at least two hours apart with a total of 1140 cGy using a Cesium137 GammaCell40 Irradiator (MDS Nordia, Kanata, ON, Canada). Primary transplants were performed with 300,000 unfractionated recipient bone marrow cells for radioprotection.

Flow cytometry

HSCs were analyzed and isolated as previously described [19]. $CD150^{+}CD41^{-}CD48^{-}Sca1^{+}c\text{-}kit^{+}$ HSCs were isolated using anti-CD150 (TC15-12F12.2-PE; BioLegend, San Diego, CA), anti-CD41 (MWReg30-FITC; BD Pharmingen, San Diego, CA), anti-CD48 (HM48-1-FITC; BioLegend), anti-Sca-1 (E13-6.7-APC), and anti-c-kit (2B8-biotin, eBiosciences, San Diego, CA), followed by Streptavidin APC-Cy7. HSCs were enriched using an AutoMacs (Miltenyi, Auburn, CA) with anti-biotin paramagnetic beads. The medium was supplemented with 200μM verapamil and 200μM chloroquine (Sigma) and incubated at 37°C for 10 minutes. An equal volume of pre-warmed deionized water with or without 200μM FDG was added to the cells and incubated at 37°C for 5 minutes. The reaction was terminated by addition of 5 volumes of ice cold staining medium with verapamil and chloroquine. All analyses excluded dead cells that stained positively for DAPI (1μg/ml) (Sigma, St. Louis, MO).

For staining of gut neural crest cells, outer muscle/plexus layer cells from the gut were dissected and dissociated as described below. Cells were stained with antibodies against p75 (Millipore, Billerica, MA) and CD49b (eBioscience, DX5). Cells were analyzed and sorted with FACS Vantage SE, FACS Aria, or FACS Canto II flow-cytometers (BD Biosciences).

Cell cycle status was determined in hematopoietic cells by using DAPI to stain DNA content. Stained hematopoietic cells were fixed in CytoFix/Cytoperm (BD Biosciences) and stained with 5 μg/ml DAPI. APC-Annexin V (BD biosciences) was used to quantify apoptotic cells following the manufacturer's instructions.

ROS levels were measured by incubating 2×10^{6} antibody stained hematopoietic cells with 5 μM 2′-7′-dichlorofluorescein diacetate (DCFDA, Molecular Probes, Eugene, OR) for 15 min at 37°C. Mitochondrial mass was measured by incubating 2×10^{6} cells with 1 nM Mitotracker Deep Red (Molecular Probes) and 50μM verapamil (Sigma) for 15 min at 37 °C. Mitochondrial membrane potential was measured by incubating 2×10^{6} cells with 25 nM

TMRM for 15 min at 37°C. Freshly isolated VZ cells were stained for 5 min at 37°C with vital dyes to preserve viability.

Colony formation assays

Four hundred live neonatal liver or spleen cells, or single HSCs were sorted per well of a 96 well plate (Corning, Corning, NY) containing 100μl of MethoCult M3434 medium (StemCell Technologies). The medium was supplemented with 1% penicillin/streptomycin, 10ng/ml Flt-3, and 10ng/ml thrombopoietin (R&D Systems). Colonies were counted after 12 days incubation at 37°C in 6% CO_2. We analyzed 32 wells per sample.

Quantitative (real-time) RT-PCR

Cells were harvested or sorted into trizol and RNA was isolated using an RNeazy Mini Kit (Qiagen Sciences, MD). cDNA was made with oligo dT primers and SuperScript II reverse transcriptase (Invitrogen). Quantitative PCR was performed with cDNA from using a SYBR Green Kit and a LightCycler 480 (Roche). Each sample was normalized to β-actin and amplification products were tested for specificity by analyzing melting curves, band size by gel electrophoresis, and amplicon sequencing.

CNS stem cell culture, differentiation and self-renewal assays

CNS and PNS cells were dissociated and cultured as previously described[27]. To isolate CNS VZ cells, ventricular zone cells were dissected from the lateral wall of the lateral ventricle of newborn *Prdm16*$^{LacZ/LacZ}$, *Prdm16*$^{LacZ/+}$ and *Prdm16*$^{+/+}$ mice. The cells were dissociated in 1ml of a 1:4 mixture of 0.025% trypsin/EDTA (Calbiochem, San Diego, CA) and Ca-, Mg-free HBSS for 4 min at 37°C. Dissociation was quenched with 2 volumes of L15 medium containing 10 mM HEPES (pH 7.4), 1 mg/ml BSA, and 25 μg/ml DNAse1. For non-adherent cultures, cells were plated at 1000 cells per well in 1.5 ml of self-renewal medium in ultra low binding six-well plates (Corning). Self-renewal medium contained a 5:3 mixture of DMEM low glucose and neurobasal medium, 1 μg/ml penicillin/streptomycin (GIBCO), 10% chick embryo extract (CEE), 2% B27 supplement, 1% N2 supplement (GIBCO), 50 μM 2-mercaptoethanol, 20 ng/ml bFGF, and 20 ng/ml EGF (R&D Systems). After 9 days culture in self-renewal medium single neurospheres larger than 50 μm in diameter were counted and transferred into differentiation medium for another 8–10 days. The differentiation phase of the culture was performed adherently in 48 well plates (1 neurosphere per well) coated with 150 μg/ml poly-D-lysine (Biomedical Technologies, Sloughton, MA) and 20μg/ml laminin (Invitrogen). Differentiation medium was the same as self-renewal medium except that it contained 5% fetal bovine serum (FBS) instead of CEE, no EGF, and 10ng/ml of bFGF instead of 20 ng/ml. Differentiated colonies were tested for multipotency by staining with neuron (Tuj1, Covance, Princeton, NJ), astrocyte (GFAP, Sigma) and oligodendrocyte (O4) markers as described in the immunochemistry section below.

To assay self-renewal potential, individual primary neurospheres (>50μm in diameter) were dissociated and re-plated at clonal density in non-adherent secondary cultures. Secondary neurospheres were counted 7–9 days later and transferred to adherent cultures containing differentiation medium to assess their ability to undergo multilineage differentiation as

described above. Self-renewal was quantified as the number of multipotent secondary colonies that were subcloned per primary neurosphere.

CNS tissue processing and immunochemistry

Newborn mouse brains were fixed in 4% paraformaldehyde, cryoprotected in 30% sucrose, embedded in Cryo-Gel embedding medium (Instrumedics, St. Louis, MO) and flash frozen. 40 μm floating sections were collected and stained with anti-β-galactosidase (ab9361, Abcam, Cambridge, MA), anti-Nestin (MAB353, Millipore, Billerica, MA) anti-phospho-Histone H3 (3H10, Millipore), anti-Tuj1 (Covance, Princeton, NJ), or anti-GFAP (DAKO) primary antibodies followed by Alexa-Fluor 488 Alexa-Fluor 594 secondary antibodies (Invitrogen). Sections were counterstained with 1 μg/ml 4′,6-diamidino-2-phenylindole (DAPI) then mounted with ProLong antifade reagent (Invitrogen).

To assess the differentiation of CNS cultures, live cells were stained with an antibody against O4 (mouse ascites, Developmental Studies Hybridoma Bank, University of Iowa), fixed with 5% acetic acid in ethanol, labeled with donkey anti-mouse IgM secondary antibody conjugated to horseradish peroxidase (HRP) (Jackson Immunoresearch) and visualized by nickel-diaminobenzidine staining. Neurons and astrocytes were labeled with the primary antibodies to Tuj1 (MMS-435P, Covance) and GFAP (G3893 Sigma), followed by Alexa-Fluor 488 goat anti-mouse IgG1 (Invitrogen) and Alexa-Fluor 555 goat anti-mouse IgG2a (Invitrogen). To assess the differentiation of PNS cultures, colonies were fixed in 5% acetic acid in ethanol for 20 min at −20°C, washed, blocked and labeled with antibodies against peripherin, (Chemicon International), GFAP and SMA (Sigma).

NAC and HGF administration

For in vitro experiments, N-acetyl-cysteine (NAC, Sigma) was added to the culture medium at a concentration of 50μM. For in vivo administration of NAC, freshly made NAC (10mg/ml in PBS, pH. 7.4) was subcutaneously injected daily into pregnant *Prdm16*$^{LacZ/+}$ mice at a dose of 67mg/kg. Pregnant mice were treated with NAC for the last 5 to 8 days of their pregnancy in most experiments but for the entire pregnancy in some experiments. To assess the effect of HGF on cultured neurospheres, CNS cells were cultured with or without 25 ng/ml HGF (R&D Systems) added to culture medium lacking CEE. Neurospheres were counted after 9 or 10 days culture, photographed to measure neurosphere diameter, and differentiated in adherent cultures as described above to assess multipotency.

Microarray analysis

Total RNA was extracted from freshly isolated VZ cells from 3 *Prdm16*$^{+/+}$, *Prdm16*$^{LZ/+}$ and *Prdm16*$^{LZ/LZ}$ neonatal brains using Trizol with 25μg/ml linear acrylamide (Ambion, Austin, TX) and treated with 2 Units of RNase-free recombinant DNase I (Ambion) to remove any contaminating genomic DNA. Purified RNA was reverse transcribed and amplified using the WT-Ovation™ Applause WT/Amp RNA amplification system (NuGEN Technologies, San Carlos, CA) following the manufacturer's instructions. Sense strand cDNA was fragmented and labeled using the FL-Ovation™ cDNA Biotin Module V2 (NuGEN). 2.5μg of labeled cDNA were hybridized to Affymetrix Mouse Gene ST 1.0 microarrays. The chips were hybridized and scanned according to the manufacturer's

instructions. Expression values for all genes were calculated using the robust multi-array average (RMA) method [28]. For the identification of genes with differential expression levels between groups, the raw expression data were analyzed using Expander v5.1 software [29], and genes with fold changes greater than 2 and p-values less than 0.05 (t-test, using log2 transformed expression values) between sample groups were considered to be significantly changed.

Chromatin immunoprecipitation

Chromatin immunoprecipitation was performed using the Magna ChIP (Millipore) kit according to the manufacturer's protocol. Briefly, neurospheres from newborn *Prdm16*$^{+/+}$ or *Prdm16*$^{LacZ/LacZ}$ littermates were grown for 9–10 days, cross-linked with 1% paraformaldehyde for 10 min, washed, and then lysed in buffer with protease inhibitor cocktail. Sonicated nuclear extracts were immunoprecipitated overnight at 4°C with anti-Prdm16 antibody (Abcam), IgG Isotype negative control antibody, or anti-Acetyl-H3-K9 (Cell Signaling) positive control antibody and Magna ChIP magnetic beads. Nuclear extracts from 3–5×10^5 cells were used per immunoprecipitation reaction. Eluted DNA and input control was purified and quantitated by qPCR. Primers were designed using Primer3 software as follow: *Hgf_1:* 5′-AGTCCAACGGGTCTCAAGTG-3′, 5′-AGTCAAGGCACAGGCAGAAC-3′; *Hgf_2:* 5′-TGCCTTCCCCTTCTCTTTCT-3′, 5′-CACTTTGCATCTCCCTGACA-3′; *Hgf_3:* 5′-TACGGGGAAACTGCTTCCTA-3′, 5′-GATCTCTTCACCCTCCTCCA-3′; *Hgf_4:* 5′-CATGTTGCTCTGTCTTATTTCAA-3′, 5′-CCCGCCCATTTTCCTATTAT-3′; *Mt2_1:* 5′-GAACACTCCAACCAGCGTTT-3′, 5′-GCGACCTTTATAGCGGAGAG-3′, *Mt2_2:* 5′-GTGGGGAAACACCATGTACC-3′, 5′-AGACCCTGCGTACAGGAAAA-3′; *Mt2_3*: 5′-CTGGCGGATACATCCAGTCT-3′, 5′-CTGAGGGGAAGGGTGGAG-3′; *Mt2_4:* 5′-CAGGATTTGTCTTTCTGGAAGC-3′, 5′-TCCCGTAAATTCATGGAGGT-3′.

Statistical analysis

All data were analyzed by homoscedastic t-tests except as noted.

Accession number

Microarray data files are available at the GEO repository (www.ncbi.nlm.nih.gov/geo/) under accession number GSE23406.

Supplementary Material

Refer to Web version on PubMed Central for supplementary material.

Acknowledgments

This work was supported by the Howard Hughes Medical Institute and by the National Institutes of Neurological Disease and Stroke (NS40750). SC was supported by a career development award from the Leukemia and Lymphoma Society. BPL was supported by an American Heart Association Postdoctoral Fellowship (0725726Z) and an Irvington Institute-Cancer Research Institute/Edmond J. Safra Memorial Fellowship. Flow-cytometry was partially supported by the UM-Comprehensive Cancer, NIH CA46592. We thank Martin White and David Adams for flow-cytometry assistance, George Wendt for technical assistance, and Elizabeth Smith (Hybridoma Core Facility) for antibody production, partially supported through the Rheumatic Core Disease Center (P30 AR48310).

References

1. Morishita K. Leukemogenesis of the EVI1/MEL1 gene family. International journal of hematology. 2007; 85:279–286. [PubMed: 17483069]
2. Bjork BC, Turbe-Doan A, Prysak M, Herron BJ, Beier DR. Prdm16 is required for normal palatogenesis in mice. Human molecular genetics. 2010; 19:774–789. [PubMed: 20007998]
3. Seale P, et al. PRDM16 controls a brown fat/skeletal muscle switch. Nature. 2008; 454:961–967. [PubMed: 18719582]
4. Seale P, et al. Transcriptional control of brown fat determination by PRDM16. Cell metabolism. 2007; 6:38–54. [PubMed: 17618855]
5. Murholm M, et al. Dynamic regulation of genes involved in mitochondrial DNA replication and transcription during mouse brown fat cell differentiation and recruitment. PloS one. 2009; 4:e8458. [PubMed: 20107496]
6. He S, Nakada D, Morrison SJ. Mechanisms of stem cell self-renewal. Annual review of cell and developmental biology. 2009; 25:377–406.
7. Miyamoto K, et al. Foxo3a is essential for maintenance of the hematopoietic stem cell pool. Cell stem cell. 2007; 1:101–112. [PubMed: 18371339]
8. Paik JH, et al. FoxOs cooperatively regulate diverse pathways governing neural stem cell homeostasis. Cell stem cell. 2009; 5:540–553. [PubMed: 19896444]
9. Renault VM, et al. FoxO3 regulates neural stem cell homeostasis. Cell stem cell. 2009; 5:527–539. [PubMed: 19896443]
10. Tothova Z, et al. FoxOs are critical mediators of hematopoietic stem cell resistance to physiologic oxidative stress. Cell. 2007; 128:325–339. [PubMed: 17254970]
11. Valk-Lingbeek ME, Bruggeman SW, van Lohuizen M. Stem cells and cancer; the polycomb connection. Cell. 2004; 118:409–418. [PubMed: 15315754]
12. Rossi DJ, Jamieson CH, Weissman IL. Stems cells and the pathways to aging and cancer. Cell. 2008; 132:681–696. [PubMed: 18295583]
13. Goyama S, et al. Evi-1 is a critical regulator for hematopoietic stem cells and transformed leukemic cells. Cell stem cell. 2008; 3:207–220. [PubMed: 18682242]
14. Kim I, Saunders TL, Morrison SJ. Sox17 dependence distinguishes the transcriptional regulation of fetal from adult hematopoietic stem cells. Cell. 2007; 130:470–483. [PubMed: 17655922]
15. Barker N, et al. Identification of stem cells in small intestine and colon by marker gene Lgr5. Nature. 2007
16. Jaks V, et al. Lgr5 marks cycling, yet long-lived, hair follicle stem cells. Nature genetics. 2008; 40:1291–1299. [PubMed: 18849992]
17. Du Y, Jenkins NA, Copeland NG. Insertional mutagenesis identifies genes that promote the immortalization of primary bone marrow progenitor cells. Blood. 2005; 106:3932–3939. [PubMed: 16109773]
18. Deneault E, et al. A functional screen to identify novel effectors of hematopoietic stem cell activity. Cell. 2009; 137:369–379. [PubMed: 19379700]
19. Kiel MJ, Yilmaz OH, Iwashita T, Terhorst C, Morrison SJ. SLAM Family Receptors Distinguish Hematopoietic Stem and Progenitor Cells and Reveal Endothelial Niches for Stem Cells. Cell. 2005; 121:1109–1121. [PubMed: 15989959]
20. Kiel MJ, Yilmaz OH, Morrison SJ. CD150- cells are transiently reconstituting multipotent progenitors with little or no stem cell activity. Blood. 2008; 111:4413–4414. [PubMed: 18398056]
21. Ren T, Zhang J, Plachez C, Mori S, Richards LJ. Diffusion tensor magnetic resonance imaging and tract-tracing analysis of Probst bundle structure in Netrin1- and DCC-deficient mice. J Neurosci. 2007; 27:10345–10349. [PubMed: 17898206]
22. West AK, Hidalgo J, Eddins D, Levin ED, Aschner M. Metallothionein in the central nervous system: Roles in protection, regeneration and cognition. Neurotoxicology. 2008; 29:489–503. [PubMed: 18313142]

23. Ozaki M, Haga S, Zhang HQ, Irani K, Suzuki S. Inhibition of hypoxia/reoxygenation-induced oxidative stress in HGF-stimulated antiapoptotic signaling: role of PI3-K and Akt kinase upon rac1. Cell death and differentiation. 2003; 10:508–515. [PubMed: 12728249]

24. Yoon YS, Lee JH, Hwang SC, Choi KS, Yoon G. TGF beta1 induces prolonged mitochondrial ROS generation through decreased complex IV activity with senescent arrest in Mv1Lu cells. Oncogene. 2005; 24:1895–1903. [PubMed: 15688038]

25. Balaban RS, Nemoto S, Finkel T. Mitochondria, oxidants, and aging. Cell. 2005; 120:483–495. [PubMed: 15734681]

26. Liu J, et al. Bmi1 regulates mitochondrial function and the DNA damage response pathway. Nature. 2009; 459:387–392. [PubMed: 19404261]

27. Nishino J, Kim I, Chada K, Morrison SJ. Hmga2 promotes neural stem cell self-renewal in young but not old mice by reducing p16Ink4a and p19Arf Expression. Cell. 2008; 135:227–239. [PubMed: 18957199]

28. Irizarry RA, et al. Exploration, normalization, and summaries of high density oligonucleotide array probe level data. Biostatistics. 2003; 4:249–264. [PubMed: 12925520]

29. Shamir R, et al. EXPANDER--an integrative program suite for microarray data analysis. BMC Bioinformatics. 2005; 6:232. [PubMed: 16176576]

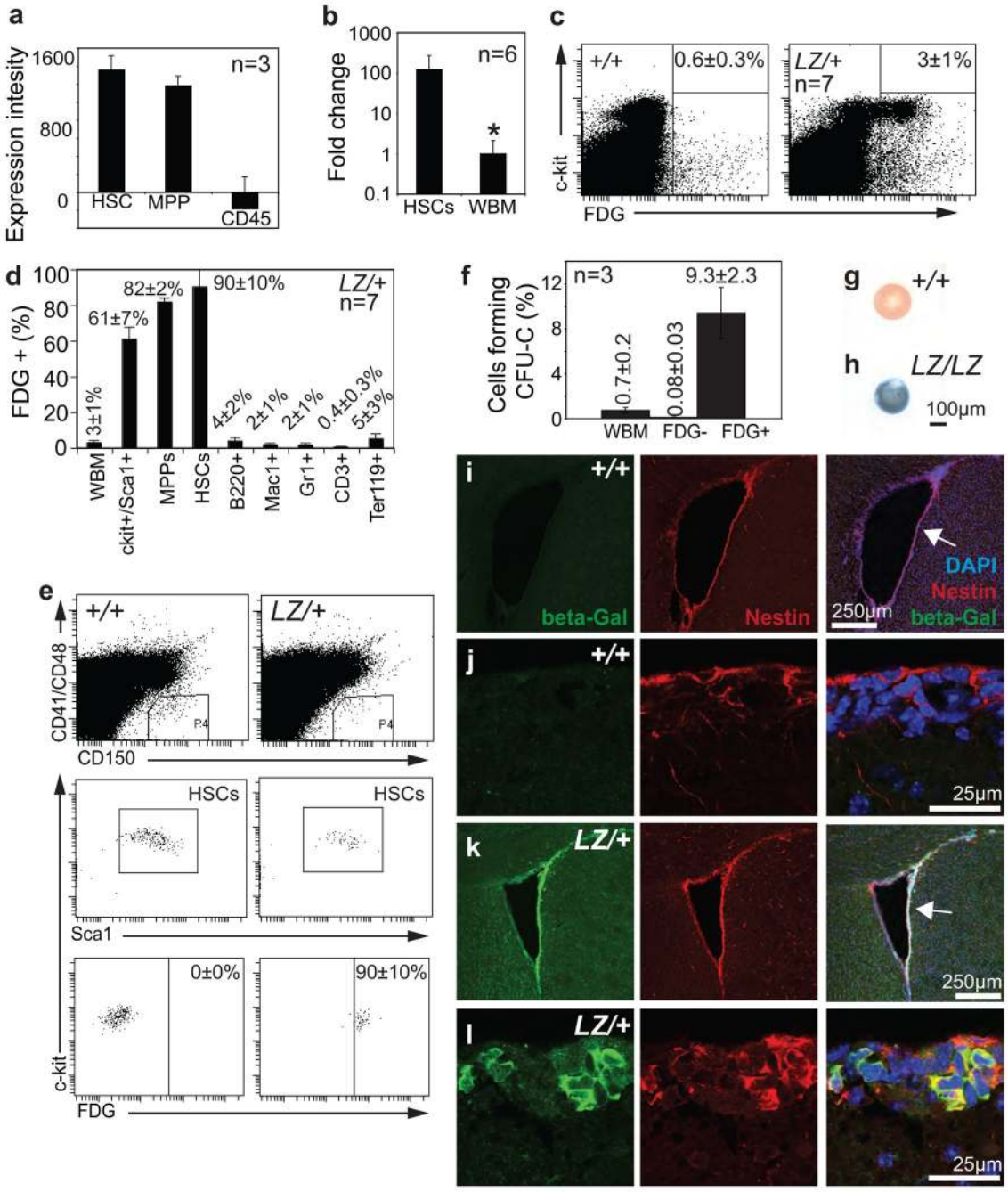

Figure 1. *Prdm16* is preferentially expressed by stem cells and primitive progenitors in the hematopoietic and nervous systems

a) Expression intensity for *Prdm16* in HSCs, non-self-renewing multipotent progenitors (MPPs) and CD45$^+$ bone marrow cells from young adult mice (data were extracted from a microarray analysis in an earlier study[19]). **b**) Quantitative RT-PCR of cDNA from CD150$^+$CD48$^-$CD41$^-$Sca1$^+$c-kit$^+$ HSCs and unfractionated bone marrow cells from young adult mice in three experiments confirmed *Prdm16* is expressed at 100-fold higher levels in HSCs. Samples were normalized using *β-actin* (*, P=0.029). **c**) FDG staining for β-

galactosidase activity in cells from 2–6 month-old *Prdm16*$^{LacZ/+}$ mice indicated that only 3±1% (mean±SD) of bone marrow cells expressed *Prdm16*. Background staining was observed in 0.6±0.3% of control bone marrow cells. Most of the bone marrow cells from *Prdm16*$^{LacZ/+}$ mice that had β-galactosidase activity were c-kit^{+}. **d, e**) The vast majority of CD150^{+}CD48^{-}CD41^{-}Sca1^{+}c-kit^{+} HSCs (90±10%; the same surface markers were used to isolate HSCs in subsequent figures) and CD150^{-}CD48^{-}CD41^{-}Sca1^{+}c-kit^{+} MPPs (82±2%; the same surface markers were used to isolate MPPs in subsequent figures) but few differentiated hematopoietic cells had β-galactosidase activity in *Prdm16*$^{LacZ/+}$ mice. **f**) FDG+ bone marrow cells from *Prdm16*$^{LacZ/+}$ adult mice were significantly ($p<0.00005$) enriched for colony-forming cells (CFU-C) in methylcellulose cultures and contained nearly all colony-forming cells in the bone marrow. The number of independent replicates is indicated in each panel that includes data from multiple independent experiments, and all error bars represent SD. Statistical significance was always assessed by Student's t-test. **g–h**) Neurospheres cultured from lateral ventricle VZ cells from newborn *Prdm16*$^{+/+}$ (**g**) or *Prdm16*$^{LacZ/LacZ}$ (**h**) mice and stained with X-gal (blue) revealed that virtually all *Prdm16*$^{LacZ/LacZ}$ neurospheres expressed *Prdm16*. **i–l**) Antibody staining for β-galactosidase indicated *Prdm16* was expressed in the adult VZ in a pattern that overlaps with the stem/progenitor cell marker Nestin.

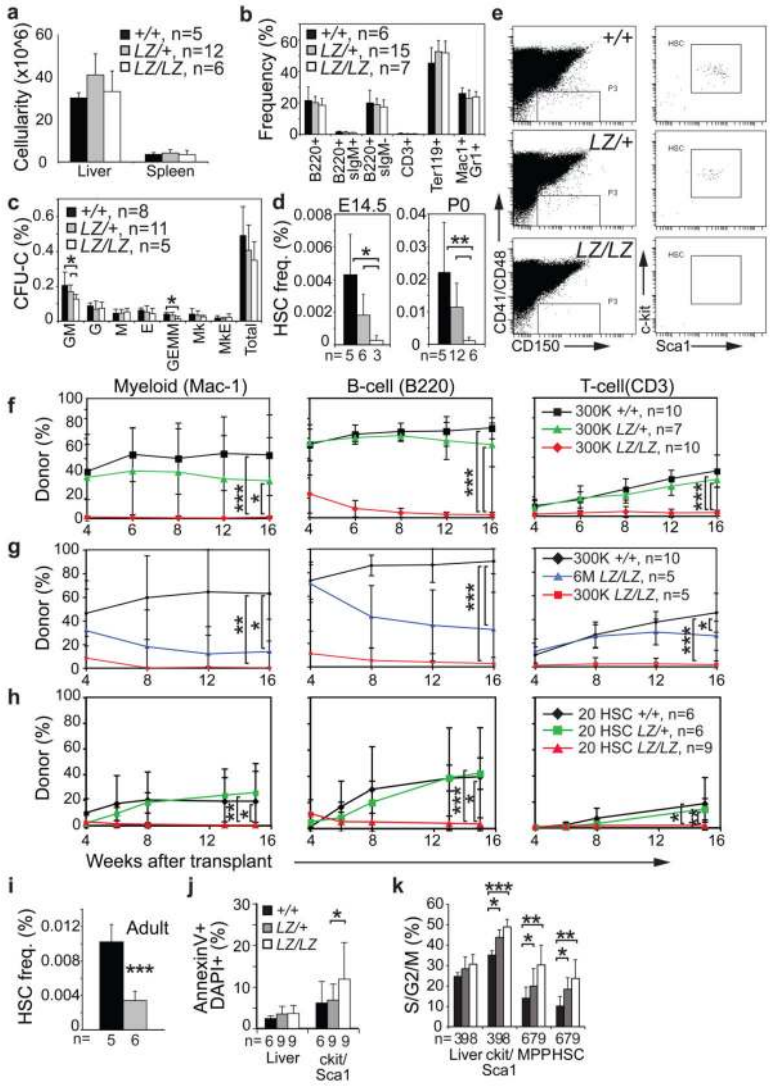

Figure 2. *Prdm16* is required for survival, cell cycle regulation, and maintenance in fetal and adult HSCs

a) The cellularity of the liver and spleen and **b)** the frequencies of mature hematopoietic cells in the liver were normal in newborn *Prdm16*$^{LacZ/LacZ}$ mice (3 independent experiments with a total of 5–12 mice/genotype; the exact number of mice is indicated in the panel legend). **c**) The frequencies of most colony-forming progenitors were normal in the liver of *Prdm16*$^{LacZ/LacZ}$ mice, but CFU-GEMM and CFU-GM were significantly depleted. **d**) HSCs were depleted in the fetal (E14.5) and newborn (P0) liver of *Prdm16*$^{LacZ/LacZ}$ mice (4 independent experiments with a total of 3–12 mice/genotype; the exact number of mice is indicated under each bar). **e**) c-kit and Sca-1 staining is shown in the right column for CD150^{+}CD48^{-}CD41^{-} cells gated in the left column for representative mice of each genotype. **f**) Irradiated CD45.1^{+} recipient mice were competitively reconstituted with 3×10^{5} CD45.2^{+} neonatal liver cells from *Prdm16*$^{+/+}$ (black lines), *Prdm16*$^{LacZ/+}$ (green lines) or *Prdm16*$^{LacZ/LacZ}$ mice (red lines) along with 3×10^{5} CD45.1^{+} recipient bone marrow cells. Each line represents average donor cell reconstitution levels (mean±SD; 3 independent

experiments with 2–5 recipients/treatment/experiment; the total number of mice transplanted with cells of each genotype is inducted in panel legends for **f–h**). **g**) Donor cell reconstitution in an independent experiment in which recipients were transplanted with 3×10^5 CD45.2$^+$ neonatal liver cells from a *Prdm16*$^{+/+}$ donor (black lines), or 3×10^5 cells from a *Prdm16*$^{LacZ/LacZ}$ donor (red lines), or 6×10^6 cells from *Prdm16*$^{LacZ/LacZ}$ donor (blue lines) along with 3×10^5 young adult CD45.1$^+$ bone marrow cells (1 experiment with at least 5 recipients/treatment). **h**) Donor cell reconstitution in 2 experiments in which recipients were transplanted with 20 CD45.2$^+$ HSCs from *Prdm16*$^{+/+}$ (black lines), *Prdm16*$^{LacZ/+}$ (green lines), or *Prdm16*$^{LacZ/LacZ}$ donors (red lines) along with 3×10^5 CD45.1$^+$ bone marrow cells (2 independent experiments). **i)** Bone marrow HSC frequency in adult *Prdm16*$^{+/+}$ and *Prdm16*$^{LacZ/+}$ mice (2 experiments with 5 or 6 mice/genotype). **j)** The frequency of annexin V+/DAPI+ unfractionated newborn liver cells or c-kit$^+$Sca-1$^+$ cells (5 independent experiments with 6 or 9 mice/genotype). **k)** Cell cycle distribution of cells from newborn liver (3 independent experiments with 3–9 mice/genotype). In panels **i–k**, the exact number of mice of each genotype is indicated under each bar in each panel (*, P<0.05; **, P<0.01; ***, P<0.001, error bars always represent SD).

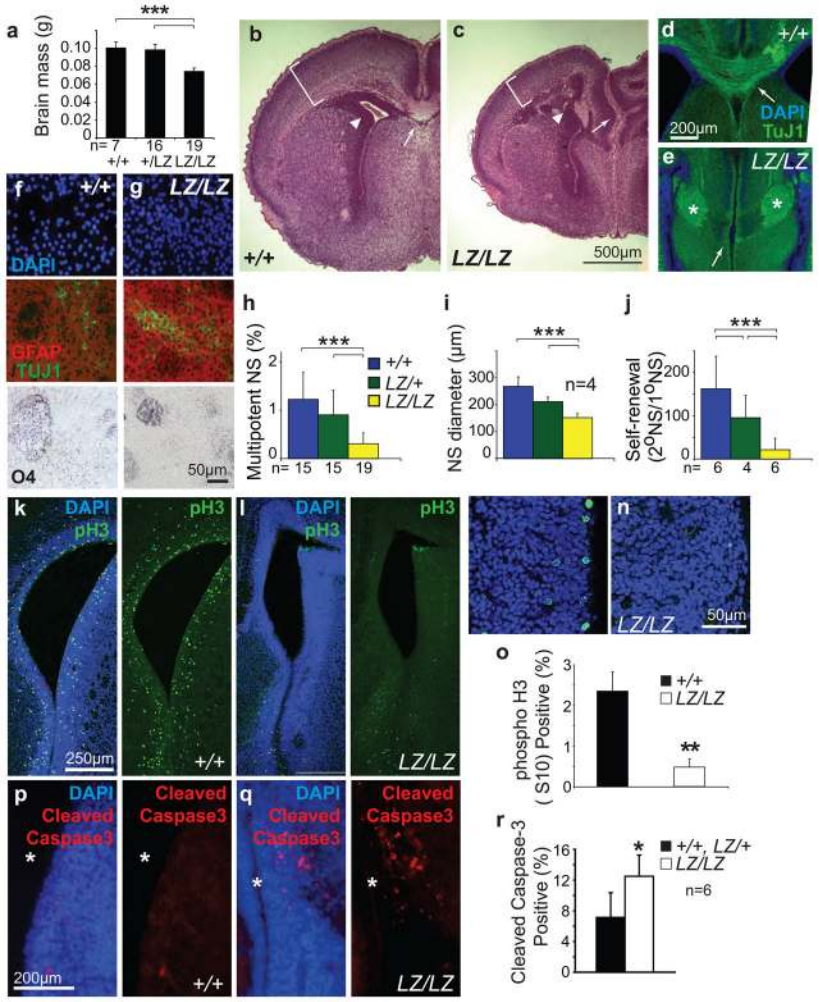

Figure 3. *Prdm16* is required for survival, cell cycle regulation, and self-renewal in neural stem cells

a) The brains of neonatal *Prdm16*$^{LacZ/LacZ}$ mice were significantly smaller than those of *Prdm16*$^{+/+}$ or *Prdm16*$^{LacZ/+}$ mice (the number of mice of each genotype is shown under each bar). **b–c)** Hematoxylin and eosin staining of coronal sections showed that *Prdm16*$^{LacZ/LacZ}$ brains (**c**) were smaller and that morphology was disrupted relative to control brains (**b**). Brackets show reduced cortical thickness, arrowheads show narrower lateral ventricle, and arrows point to the lack of a corpus callosum in the *Prdm16*$^{LacZ/LacZ}$ brain. **d–e)** Agenesis of the corpus callosum was confirmed by staining with the neuronal marker TuJ1 which revealed axon tracts that crossed the midline in wild-type (arrow, **d**) but Probst bundles that did not cross the midline in *Prdm16*$^{LacZ/LacZ}$ brains (*, **e**). **f–j)** Some primary neurospheres of all genotypes underwent multilineage differentiation, forming neurons (TuJ1+), astrocytes (GFAP+), and oligodendrocytes (O4+); however, a significantly lower percentage of VZ cells from newborn *Prdm16*$^{LacZ/LacZ}$ mice formed multipotent neurospheres compared to littermate controls (**h**) and the diameter (**i**) and self-renewal potential (**j**) of *Prdm16*$^{LacZ/LacZ}$ neurospheres was significantly less than control neurospheres (the number of mice per genotype is indicated in each panel; panels **h, i**, and **j**

reflect 6, 4, and 3 independent experiments). Self-renewal was quantified as the number of multipotent secondary neurospheres generated upon the subcloning of individual primary neurospheres. **k–o**) Significantly fewer dividing cells were observed in the VZ of newborn *Prdm16*$^{LacZ/LacZ}$ mice compared to littermate controls based on phospho-histone3 (pH3) staining (3 mice per genotype and 4 sections per mouse). **p–r)** Significantly more cells underwent cell death in the lateral ventricle VZ of newborn *Prdm16*$^{LacZ/LacZ}$ mice compared to littermate controls (* marks lateral ventricle) in sections (**p–q**), and by flow cytometry (6 mice/genotype from 3 independent experiments). (*, P<0.05; **, P<0.01; ***, P<0.001, error bars always represent SD).

a

Symbol	Description	Microarray WT/KO	Microarray HET/KO	qRT PCR WT/KO	qRT PCR HET/KO
Hgf *	hepatocyte growth factor	6.2	4.4	75±18	38±12
Lhcgr	luteinizing hormone/choriogonadotropin receptor	6.1	4.2	12±6	8.0±2.0
Luzp2	leucine zipper protein 2	4.4	3.2	ND	ND
Mt2 *	metallothionein 2	3.8	3.4	5.7±1.1	4.8±0.1
Pdk4 *	pyruvate dehydrogenase kinase, isoenzyme 4	3.7	2.8	5.0±0.2	3.0±0.6
Crym	crystallin, mu	3.2	2.2	2000±1090	675±350
Capsl	calcyphosine-like	2.8	2.3	ND	ND
Prdm16	PR domain containing 16	2.6	2.0		
Ogn	osteoglycin	2.6	2.1	27±29	18±17
Papss2	3'-phosphoadenosine 5'-phosphosulfate synthase 2	2.5	2.1	13±13	27±31
Hmgcs2	3-hydroxy-3-methylglutaryl-Coenzyme A synthase 2	2.4	2.1	10±2	10±1
Iqcg	IQ motif containing G	2.4	2.3	ND	ND
Gm70		2.2	1.9	ND	ND

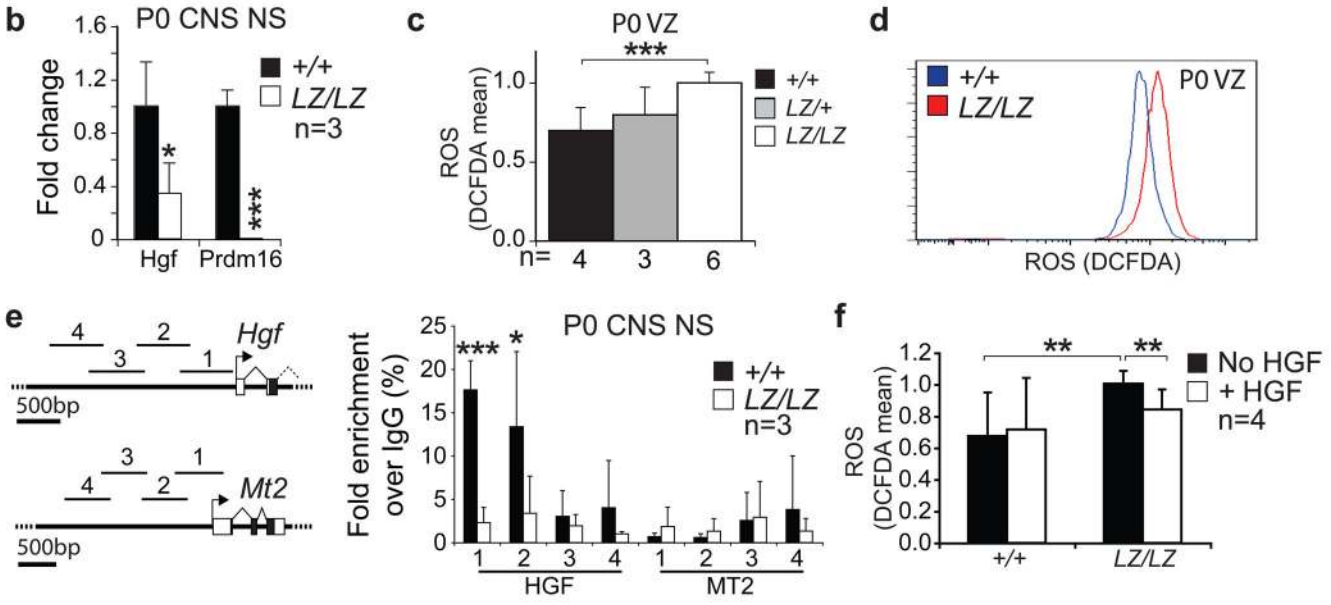

Figure 4. *Prdm16* promotes the expression of *Hgf* and regulates ROS levels in neural stem/progenitor cells

a) The gene expression profiles of VZ cells from newborn *Prdm16*$^{+/+}$, *Prdm16*$^{LacZ/+}$, and *Prdm16*$^{LacZ/LacZ}$ mice were compared by microarray (3 independent samples per genotype). The list shows all genes that were significantly ($p<0.05$) reduced in expression within *Prdm16*$^{LacZ/LacZ}$ VZ cells as compared to control cells (by at least 2.2 fold between *Prdm16*$^{+/+}$ and *Prdm16*$^{LacZ/LacZ}$ VZ and at least 1.8 fold between *Prdm16*$^{LacZ/+}$ and *Prdm16*$^{LacZ/LacZ}$ cells). Asterisks indicate genes associated with ROS regulation or response to oxidative stress. Differential expression was confirmed by qPCR in 3 independent samples/genotype. Genes that increased in expression in *Prdm16*$^{LacZ/LacZ}$ VZ cells are shown in Suppl. Fig. 3e. **d**) *Hgf* expression was confirmed to decline by qPCR in neurospheres cultured from *Prdm16*$^{LacZ/LacZ}$ mice. **c–d)** Newborn *Prdm16*$^{LacZ/LacZ}$ VZ cells had significantly and uniformly increased ROS levels based on DCFDA staining. **e**) Prdm16 bound to the promoter of *Hgf* but not *Mt2*. Chromatin immunoprecipitation was conducted using anti-Prdm16 antibodies and primary neurospheres from *Prdm16*$^{+/+}$ and *Prdm16*$^{LacZ/LacZ}$ mice. qPCR was used to quantify the immunoprecipitated *Hgf* and *Mt2*

promoter regions indicated on the schematics. Data are shown as fold enrichment over control IgG immunoprecipitation. Statistical significance was determined by paired T-tests comparing fold enrichment of target sequences immunoprecipitated by anti-Prdm16/MT2 antibody versus input DNA compared to control IgG versus input DNA. **f**) HGF treatment reduced ROS levels in neurospheres grown adherently for 5–6 days. HGF was added to the cultures 20 hours before ROS measurement. The number of independent experiments is indicated in each panel, or on each bar in panel **c** to indicate the number of experiments in which mice of the indicated genotype were used. *, P<0.05; **, P<0.01; ***, P<0.001, error bars always represent SD.

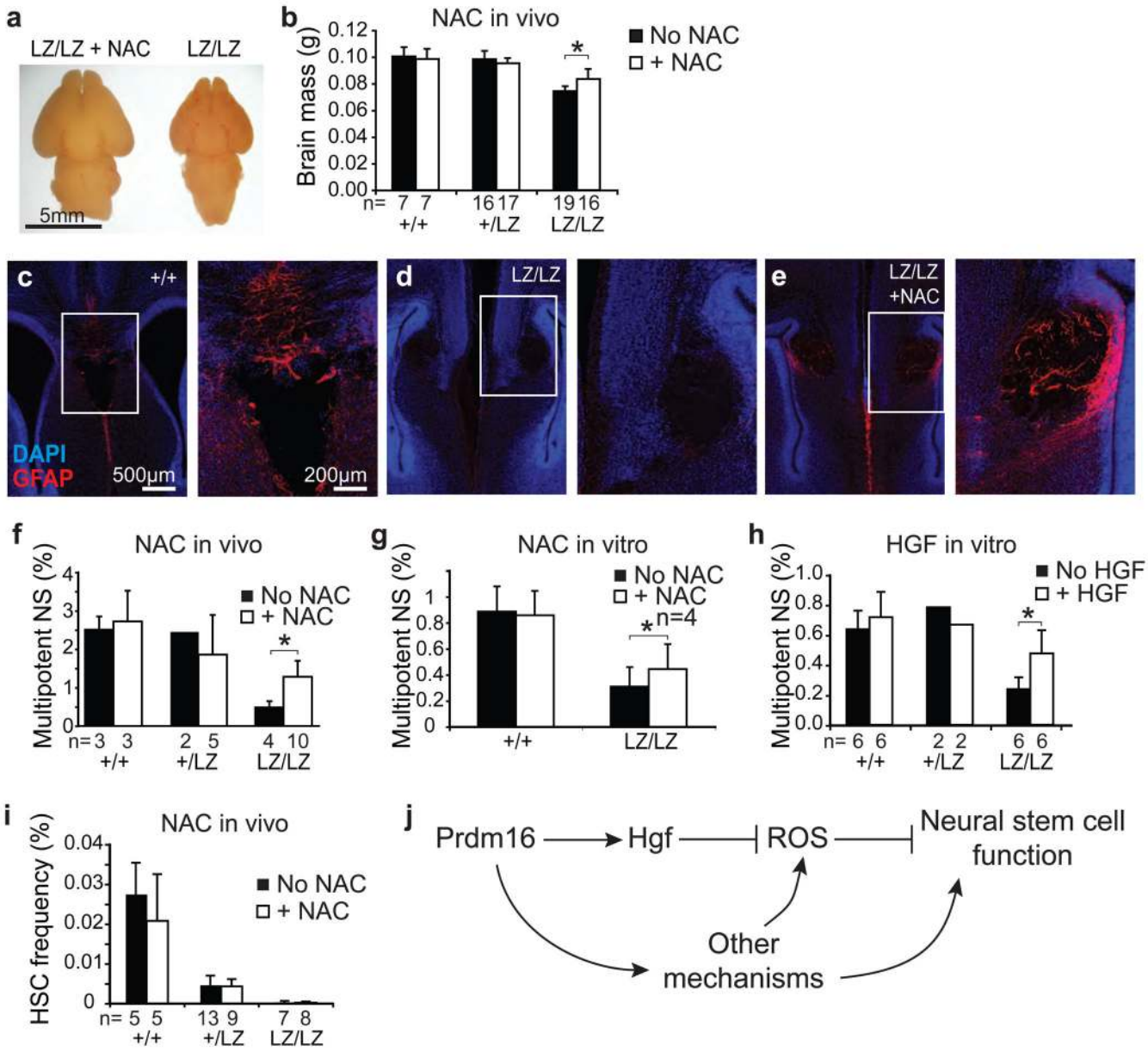

Figure 5. *Prdm16* promotes neural stem/progenitor cell function by regulating *Hgf* expression and ROS levels

NAC treatment significantly increased brain size (**a**) and mass (**b**) in *Prdm16*$^{LacZ/LacZ}$ mice but not in littermate controls (the number of mice per treatment is indicated under each bar; each panel reflects at least 3 independent experiments). **c–e**) Newborn *Prdm16*$^{LacZ/LacZ}$ mice (**d**) had reduced GFAP staining (red) in the midline relative to control littermates (**c**) but this phenotype was partially rescued by NAC treatment (**e**). Higher magnification images of the boxed regions are shown to the right. **f)** NAC treatment in utero significantly (by paired t-test) increased the percentage of newborn *Prdm16*$^{LacZ/LacZ}$ VZ cells that formed multipotent neurospheres in culture. Addition of NAC (**g**) or HGF (**h**) to culture significantly increased the percentage of newborn *Prdm16*$^{LacZ/LacZ}$ VZ cells that formed multipotent neurospheres. **i**) NAC treatment of pregnant mice did not rescue the depletion of

HSCs in *Prdm16*$^{LacZ/LacZ}$ mice. (*, P<0.05; **, P<0.01; ***, P<0.001, error bars always represent SD). j) A model of Prdm16 function in neural stem cells.